Exchange interactions in barium hexaferrite

P. Novák
Institute of Physics of ASCR, Cukrovarnická 10, 162 53 Prague 6, Czech Republic

J. Rusz
Department of Electronic Structures, Faculty of Mathematics and Physics, Charles University, Ke Karlovu 5, 121 16 Prague 2, Czech Republic
and Institute of Physics of ASCR, Cukrovarnická 10, 162 53 Prague 6, Czech Republic
(Received 30 September 2004; revised manuscript received 11 January 2005; published 31 May 2005)

The electronic structure of $BaFe_{12}O_{19}$ hexaferrite is calculated using the density functional theory and generalized gradient approximation (GGA). The GGA+U method is used to improve the description of strongly correlated 3*d* electrons of Fe. The calculation is performed for a number of spin configurations. From differences of the total energies 13 independent exchange integrals are determined as functions of the parameter *U*. Their magnitude decreases with increasing *U*, pointing to the dominating role played by the antiferromagnetic superexchange. The Curie temperature T_C is calculated using the molecular field and the random phase approximations. T_C determined by the random phase approximation agrees with the experimental T_C for $U \approx 6-7$ eV.

DOI: 10.1103/PhysRevB.71.184433 PACS number(s): 75.30.Et, 75.50.Gg

I. INTRODUCTION

M-type hexaferrites $MFe_{12}O_{19}$ ($M=Sr,Ba,Pb$) are suitable and inexpensive materials for hard magnets (for a survey of their properties, see Ref. 1). At the same time these systems represent a unique possibility to study iron in the same compound but in different ligand polyhedra, as Fe enters five different sublattices—three with octahedral, one with tetrahedral, and one with bipyramidal co-ordination. The knowledge of magnetic interactions of the iron ions on individual sublattices would significantly help in predicting the properties of substituted hexaferrites. In view of the complexity of the system, such information is difficult to obtain experimentally and theoretical analysis is thus desirable. In this paper the calculation of the exchange interaction, based on the density functional theory (DFT), in the $BaFe_{12}O_{19}$ hexaferrite is presented. A stringent check of the reliability of the calculated exchange integrals is the value of corresponding Curie temperature T_C. The molecular field approximation (MFA), commonly used to determine T_C in complex magnetic insulators, is known to overestimate its value.[2] An improvement of MFA is represented by the random phase approximation (RPA) that until now was applied to simple, single sublattice ferromagnets only. In the present paper RPA is applied to the complex ferrimagnet in question and the result is compared with that obtained by MFA.

Electronic structure of the stoichiometric strontium hexaferrite was calculated recently by Fang *et al.*[3] These authors used the localized spherical wave method employing density functional theory (DFT) and the local spin density approximation (LSDA). Besides the spin configuration that corresponds to the ground state, several other spin configurations were considered. In Sec. V these results will be discussed and compared with the results obtained in the present paper.

II. MANY-SUBLATTICE SYSTEM—EXCHANGE INTEGRALS AND TOTAL ENERGY

Assuming that the exchange interaction is isotropic and bilinear, the energy e_{12} of the pair of spins $\vec{S}_1$, $\vec{S}_2$ is

$$e_{12} = J(\vec{S}_1\vec{S}_2), \tag{1}$$

where J is the exchange integral. In the complex system with N magnetic sublattices, where only intersublattice exchange is nonzero, the exchange energy per unit cell may be then written as

$$E_{ex} = \frac{1}{2}\sum_{i=1}^{N}\sum_{j\neq i=1}^{N} n_i z_{ij} J_{ij}(\vec{S}_i\vec{S}_j), \tag{2}$$

where i, j numerate the sublattices, n_i is the number of ith sublattice sites in the unit cell, and z_{ij} is the number of sites belonging to the sublattice j that are neighbors of the site from sublattice i. $\vec{S}_i$ is the spin of the atom on the ith sublattice.

The following analysis is limited to collinear systems, but we consider different mutual arrangements of the sublattice spins. Then

$$\vec{S}_i\vec{S}_j = S_i S_j \sigma_i^{(\alpha)}\sigma_j^{(\alpha)}, \tag{3}$$

where index α labels different arrangements of the sublattice spins and $\sigma_i^{(\alpha)} = \pm 1$. E_{ex} then becomes

$$E_{ex} = \frac{1}{2}\sum_{i=1}^{N}\sum_{j\neq i=1}^{N} n_i z_{ij} J_{ij} S_i S_j \sigma_i^{(\alpha)}\sigma_j^{(\alpha)}. \tag{4}$$

The difference $\Delta^{(\alpha)}$ of the exchange energy of the excited state α and the ground state ($\alpha=0$) is

TABLE I. The Fe sublattices in hexaferrites. n_i is number of atoms belonging to the ith sublattice in the unit cell, $\sigma_i^{(0)}=1$ (-1) denotes that in the ground state the spin of the ith sublattice is up (down).

Index	Denomination	Polyhedron	n_i	$\sigma_i^{(0)}$
1	a	octahedron	2	+1
2	b	bipyramid	2	+1
3	f_1	tetrahedron	4	−1
4	f_2	octahedron	4	−1
5	k	octahedron	12	+1

$$\Delta^{(\alpha)}=\frac{1}{2}\sum_{i=1}^{N}\sum_{j\neq i=1}^{N} n_i z_{ij} J_{ij} S_i S_j (\sigma_i^{(\alpha)}\sigma_j^{(\alpha)}-\sigma_i^{(0)}\sigma_j^{(0)}). \quad (5)$$

First we consider an arrangement in which the spin $\vec{S}_i$ of a single sublattice is inverted relative to the ground state and denote $\Delta^{(\alpha)}\equiv\Delta_i$:

$$\Delta_i=-2S_i n_i \sum_{j\neq i} z_{ij} J_{ij} S_j \sigma_i^{(0)}\sigma_j^{(0)}. \quad (6)$$

Second, an arrangement corresponding to spins $\vec{S}_i$, $\vec{S}_j$ of two sublattices inverted relative to the ground state is considered. Denoting $\Delta^{(\alpha)}\equiv\Delta_{ij}$ we obtain

$$\Delta_{ij}=\Delta_i+\Delta_j+4n_i z_{ij} J_{ij} S_i S_j \sigma_i^{(0)}\sigma_j^{(0)}. \quad (7)$$

Note that $n_i z_{ij}=n_j z_{ji}$. With known S_i, and n_i, z_{ij} fixed by the geometry of the crystal lattice, this equation allows us to determine the exchange integral

$$J_{ij}=(\Delta_{ij}-\Delta_i-\Delta_j)/(4S_i S_j n_i z_{ij}\sigma_i^{(0)}\sigma_j^{(0)}). \quad (8)$$

The density-functional-based calculations yield the total energy and, if they could be performed for all above spin arrangements, the exchange integrals are easily determined. To make this approach useful, the exchange interaction must be short range, otherwise very large unit cells have to be considered. It is generally accepted that in ferrites this condition is fulfilled—the main mechanism is the superexchange that decreases rapidly with the increasing Fe—Fe distance (see Ref. 4 for detailed analysis).

In the above analysis we assumed that there is no intrasublattice exchange and that the spin in the ith sublattice interacts with the nearest jth neighbors only. If the intra-sublattice exchange for a specific sublattice is important, the sublattice should be subdivided so that the interacting spins are in different sub-sublattices. Similarly, if exchange integrals J_{ij} are nonzero not only for the nearest (nn) but also for the next-nearest neighbors (nnn), a subdivision is required or we have to be satisfied with determining the linear combination $z_{ij}^{nn}J_{ij}^{nn}+z_{ij}^{nnn}J_{ij}^{nnn}$ instead of J_{ij}^{nn}, J_{ij}^{nnn}.

In the hexaferrites, iron ions enter five different sublattices and in the Ba- hexaferrite the nominal valency of iron in all sublattices is 3+. The ground state of Fe^{3+} ion is ^6S corresponding to spin $S=5/2$ and orbital moment $L=0$. Zero orbital moment is of importance as it implies that the exchange interaction is isotropic to a good approximation. Basic information concerning the five iron sublattices is given in Table I, while numbers of the neighbors z_{ij} and corresponding distances r_{ij} are summarized in Table II.

TABLE II. The nearest neighbor Fe ions in $BaFe_{12}O_{19}$. z_{ij} is the number of sites belonging to the sublattice j that are neighbors of the site from sublattice i and r_{ij} is corresponding distance in nm. The data for the next-nearest neighbors are also given if r_{ij} is smaller than 0.4 nm.

	$2a$		$2b$		$4f_1$		$4f_2$		$12k$	
	z_{ij}	r_{ij}	z_{ij}	r_{ij}	z_{ij}	r_{ij}	z_{ij}	r_{ij}	z_{ij}	r_{ij}
$2a$	6	0.589	2	0.580	6	0.346	6	0.557	6	0.305
$2b$	2	0.580	6	0.589	6	0.619	6	0.367	6	0.371
$4f_1$	3	0.346	3	0.619	3	0.363	1	0.379	6	0.350
									3	0.356
$4f_2$	3	0.557	3	0.367	1	0.379	1	0.277	6	0.351
$12k$	1	0.305	1	0.371	2	0.350	2	0.351	2	0.291
					1	0.356			2	0.298

III. METHOD OF CALCULATION

All calculations were performed with the experimental crystal structure parameters[5] employing the WIEN2k program.[6] This program is based on the density functional theory and it uses the full-potential linearized augmented plane wave (FPLAPW) method with the dual basis set. In the APW-like methods the space is divided in the nonoverlapping atomic spheres and the interstitial region. The electron states are then classified as the core states, which are fully contained in the atomic spheres, and the valence states. The valence states are expanded using the basis functions; each of the basis functions has the form of a plane wave in the interstitial region, while it is an atomiclike function in the atomic spheres. To make possible treatment of two valence functions with the same orbital number (like 3p and 4p functions of Fe), so-called local orbitals are added to the basis functions.[7] In our calculations 3p, 3d, 4s, 4p states of Fe, 2s, 2p, 3s of O, and 4s, 4p, 5s, 5p of Ba are treated as valence states. The number n_k of the k points in the irreducible part of the Brillouin zone was 4. The symmetry of the crystal lattice is hexagonal with 24 symmetry operations. The unit cell comprises then 11 inequivalent sites—Ba (multiplicity 2), five iron sites (multiplicity 2,2,4,4,12), and five oxygen sites (multiplicity 4,4,6,12,12). The total number of sites in the unit cell is thus 64.

All calculations were spin polarized; for the exchange correlation potential we adopted the GGA form.[8] Single calculation with the LSDA exchange-correlation potential[9] was performed for the ground state spin structure. The radii of the atomic spheres were 2.0 a.u. for Ba, 1.9 a.u. for all five inequivalent Fe, and 1.6 a.u. for the oxygens.

Despite the fact that GGA is more suitable than LSDA when applied to inhomogeneous electron systems, in the 3d transition metal oxides the energy gap and the magnetic moments are still underestimated.[10] To improve the description

of Fe 3*d* electrons we thus used the rotationally invariant version of the LDA+U method as described by Liechtenstein *et al.*,[13] but with the GGA instead of LSDA exchange-correlation potential. The method should be therefore more correctly denoted as GGA+U. The method is no longer truly *ab initio* as the values of the Hubbard parameter U and the exchange parameter J must be inserted. These can either be taken from experiment or estimated using the restricted LSDA (GGA) calculation. In the restricted LSDA calculations for octahedrally coordinated Fe^{3+} ion in $LaFeO_3$ (Ref. 11) $U=9.3$ eV was obtained, while a smaller value $U(Fe^{3+})=5.5$ eV was deduced from the photoemission and inverse photoemission experiments on α-Fe_2O_3.[12] The exchange parameter J is believed to be close to its atomic value $J\sim 1$ eV.[11] In any case we can rely on reasonable limits for these parameters rather than on their specific values.

In the LDA+U methods an orbitally dependent potential is introduced for the chosen set of electron states, which in our case are 3*d* states of Fe. The additional potential has an atomic Hartree-Fock form, but with screened Coulomb and exchange interaction parameters. The problem is that the exchange and correlation already contained in the LSDA or GGA should be subtracted. The form of this "double counting correction" is spherically symmetrical and it is not clear to which extent its application in the full potential methods is justified, as there is no "double counting correction" for the nonspherical terms in the orbital potential. We avoided this problem by using instead of the parameter U an effective $U_{eff}=U-J$ and putting the nonspherical terms in orbital potential equal to zero. In what follows the notation $U\equiv U_{eff}$ is used, but it should be kept in mind that we are dealing with the effective U which is somewhat smaller than the Hubbard parameter as $J/U\approx 0.1-0.2$. To see how the results depend on U_{eff}, three values $U_{eff}=3.47$, 6.94, and 10.41 eV were employed in addition to the GGA calculation which corresponds to $U=0$. We note that the WIEN2k program was used recently to calculate U_{eff} of the Fe^{3+} ion in Fe_2O_3 and Fe_3O_4.[14] The values $U_{eff}=7.33$ and 7.38 eV were obtained for the octahedrally coordinated Fe^{3+} ion in Fe_2O_3 and Fe_3O_4, while smaller value 6.33 eV was calculated for the tetrahedral Fe^{3+} ion in Fe_3O_4.

To check whether the number n_k of the k points in the irreducible part of the Brillouin zone and the size of the basis yield sufficiently accurate results, additional calculations using the GGA ($U=0$) were made, as in this case the system is metallic for most of the excited configurations and thus the results are more sensitive comparing to $U\neq 0$ calculations, for which the gap always exists. n_k was increased from 4 to 7 and the number of basis functions n_B from 4160 to 5220. While the change of the total energy itself is appreciable, the differences of the total energies from which the exchange integrals are calculated are rather insensitive. Their typical change was a few percent, with the maximal change 7.3%. For the GGA+U calculations the changes should be smaller and we thus concluded that the lower values of n_k and n_B are sufficient.

IV. RESULTS

A. Ground state spin arrangement

The total density of states (DOS) for the ground state spin arrangement calculated with LSDA, GGA, and GGA+U ($U=6.94$ eV) is displayed in Fig. 1. A metallic state, with the nonzero DOS at the Fermi energy, is predicted by the LSDA; GGA gives a state on the brink of metal and insulator. An insulating state is only obtained with the GGA+U. The magnetic moments of individual atoms, the total moment, and the gap magnitude are given in Table III. Total magnetic moment calculated with LSDA is smaller than nominal magnetic moment 40 μ_B per unit cell. The GGA gives moment closer to 40 μ_B and in all GGA+U calculations the total magnetization is very close to its nominal value—the remaining discrepancy originates from the error of the integration over the

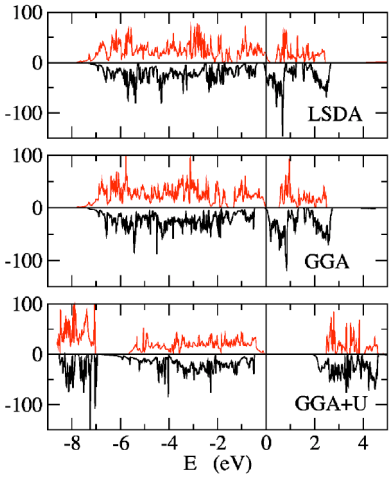

FIG. 1. The DOS (in states/eV) of $BaFe_{12}O_{19}$ hexaferrite calculated using LSDA, GGA, and GGA+U ($U=6.94$ eV) methods. Positive (negative) values correspond to majority (minority) spin states.

TABLE III. The ground spin configuration. LSDA and GGA+U calculations for four values of the parameter U ($U=0$ corresponds to the GGA). Magnetic moments inside the atomic spheres of individual nonequivalent ions, magnetic moment M of the unit cell and the gap. All magnetic moments are in units of μ_B; parameter U and the gap are in eV.

		GGA+U			
	LSDA $U=0$	$U=0$	$U=3.47$	$U=6.94$	$U=10.41$
Ba	0.0	0.0	0.0	0.0	0.0
Fe($2a$)	3.48	3.67	4.02	4.20	4.34
Fe($2b$)	3.36	3.48	3.89	4.12	4.29
Fe($4f_1$)	−3.22	−3.38	−3.87	−4.12	−4.29
Fe($4f_2$)	−3.04	−3.30	−3.95	−4.10	−4.35
Fe($12k$)	3.46	3.68	4.02	4.21	4.36
O($4e$)	0.34	0.39	0.35	0.29	0.23
O($4f$)	0.09	0.12	0.09	0.07	0.05
O($6h$)	0.08	0.07	0.04	0.02	0.01
O($12k_1$)	0.08	0.10	0.09	0.07	0.06
O($12k_1$)	0.17	0.19	0.17	0.14	0.11
M	37.73	39.93	40.01	40.01	40.01
Gap	0.0	0.0	1.07	2.11	2.70

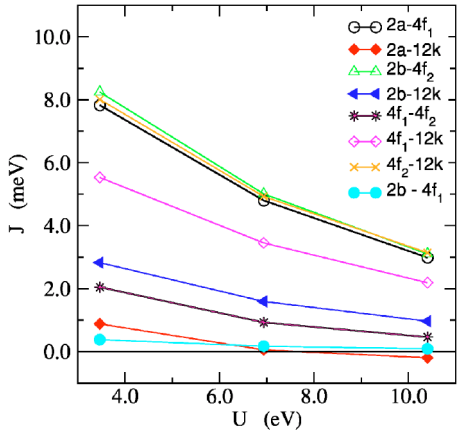

FIG. 2. (Color online) The intersublattice exchange integrals as functions of U. Exchange integrals $|J_{ab}|$ and $|J_{af_1}|$ are smaller than 0.01 eV and they are omitted.

Brillouin zone and from leaking of the core states out of the atomic spheres. The magnetic moments of Fe ions increase and moments on oxygens decrease as U is increased—this is a typical result of the LDA+U methods that tend to make the occupation of electron states integer.

B. Inter-sublattice interactions

There are five Fe sublattices, thus there are five arrangements with the spin of the single sublattice inverted and the number of arrangements with the spins of two sublattices inverted is ten. In addition the ground state must be considered. To make full use of the formula (8) 16 calculations are thus needed. Inspection of Table II shows that in the case of $4f_1-12k$ exchange the interaction between the next-nearest neighbors may be important. Fortunately the geometry of the Fe—O—Fe triad of the nearest and the next-nearest neighbors is similar ($12k$-O distances are 0.2116 and 0.2093 nm, $4f_1$-O distances 0.1894 and 0.1893 nm and the $12k$-O-$4f_1$ angle 121.3 and 126.1 deg, respectively). In what follows we neglect the difference and merge the nn and nnn putting $z_{f_1k}=9$.

When using the GGA, converged results were obtained for eight excited spin arrangements only. For six of them the total magnetic moment m_{tot} differs markedly from its nominal value, pointing to the fact that the spin inversion led to a profound change of the electron structure. This in turn is connected with the metallic character of the system. On the other hand the GGA+U calculations may be converged for all 15 excited spin arrangements and the calculated moment always equals its nominal value. The DOS exhibits a gap; its smallest value is 0.80 eV obtained for the ferromagnetic configuration and $U=3.47$ eV.

The intersublattice exchange integrals as functions of the parameter U are plotted in Fig. 2. Interactions Fe(a)-Fe(b) and Fe(a)-Fe(f_2) proved to be very small with $|J_{ab}|$, $|J_{af_2}| < 0.01$ eV and they are thus not shown.

C. Intra-sublattice interactions

Inspection of Table II reveals that the distance of neighboring sites in sublattices $4f_1$, $4f_2$, and $12k$ is smaller than 0.4 nm and in fact $4f_2$ and $12k$ sites have the nearest Fe neighbors in the same sublattice. The exchange interaction within these two sublattices cannot be thus neglected. Moreover, for the $12k$ sublattice the interaction between the next-nearest neighbors must also be considered. Similarly as for $4f_1$-$12k$ interaction the geometries of the Fe—O—Fe triads for the nearest and the next-nearest Fe neighbors are very similar and, neglecting their difference, we put $z_{kk}=4$.

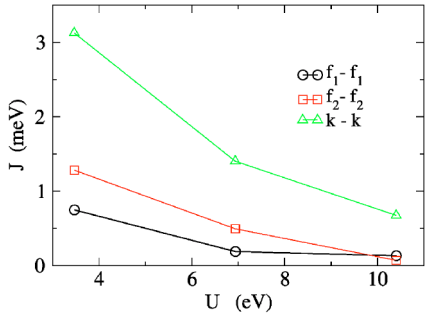

FIG. 3. (Color online) The intrasublattice exchange integrals as functions of U for $4f_1$, $4f_2$, and $12k$ sublattices.

As mentioned in Sec. II, to determine the intra-sublattice exchange we have to subdivide the sublattice in question. The subdivision lowers the symmetry of the system and the number of inequivalent sites increases which makes the calculation more costly. If possible the inversion symmetry should be preserved, as for the systems without inversion the complex instead of real eigenvalue problem must be solved. The sublattices can be divided in several different ways; the subdivision which preserves the highest symmetry should be preferred. We divided the sublattice $4f_2$ in $2f_2'$, $2f_2''$, which increased the number N_a of inequivalent atoms from 11 to 19 and reduced the number N_s of symmetry operations from 24 to 12. The inversion center is preserved. For the $12k$ sublattice we have chosen the division in $8k'$, $4k''$ sub-sublattices, which leads to $N_a=15$, $N_s=8$ and again inversion center is preserved. Finally the division of $4f_1$ in $2f_1'$, $2f_1''$ increases N_a to 18, reduces N_s to 12, and the center of inversion is lost. The results are summarized in Table V.

The three intra-sublattice exchange integrals as functions of the parameter U are plotted in Fig. 3.

V. DISCUSSION

It is seen from Tables IV and V that among all possible spin configurations it is the experimentally found spin structure that has the lowest energy. The same conclusion was also made by Fang *et al.*,[3] though only a limited number of configurations were considered by these authors. Their results are based on the localized spherical wave (LSW) method that is faster but presumably less reliable compared to the FPLAPW method used in the present paper. First, the LSW is not a full potential method as the potential is spherically averaged within the atomic spheres. Second, to fill the space, "empty atomic spheres" must be added and that is a rather arbitrary procedure. Another difference is that the local spin density approximation was employed in Ref. 3 and no attempt was made to improve the description of the elec-

TABLE IV. The energy difference $\Delta(U)$ in eV between excited spin arrangement (inverted spins of iron sublattices s_1, s_2) and the ground state. GGA+U calculation have four different U values ($U=0$ corresponds to GGA). Δ^* are the results for $SrFe_{12}O_{19}$ taken from Ref. 3. $M(0)$ is the magnetic moment of the unit cell for the GGA calculation in units of μ_B, M_n is its nominal value. The calculations with $U\neq 0$ led to M that differed from M_n by less than 0.03 μ_B. nc in the "$U=0$" column means that the calculation does not converge or that it converges to a different spin configuration.

s_1	s_2	$\Delta(0)$	$\Delta(3.47)$	$\Delta(6.94)$	$\Delta(10.41)$	Δ^*	$M(0)$	M_n
$2a$	⋯	1.378	1.035	0.708	0.477	⋯	19.99	20
$2b$	⋯	1.184	0.849	0.532	0.331	⋯	19.96	20
$4f_1$	⋯	4.871	3.600	2.251	1.425	3.77	67.91	80
$4f_2$	⋯	nc	3.545	2.190	1.389	4.86	nc	80
$12k$	⋯	6.244	4.337	2.790	1.817	⋯	−62.88	−80
$2a$	$2b$	nc	1.883	1.240	0.808	1.78	nc	0
$2a$	$4f_1$	3.458	2.286	1.518	1.006	⋯	59.50	60
$2a$	$4f_2$	nc	4.578	2.900	1.868	⋯	nc	60
$2a$	$12k$	nc	5.639	3.516	2.237	6.77	nc	−100
$2b$	$4f_1$	nc	4.371	2.747	1.737	⋯	nc	60
$2b$	$4f_2$	3.323	1.918	1.216	0.787	⋯	52.18	60
$2b$	$12k$	nc	6.036	3.802	2.440	7.22	nc	−100
$4f_1$	$4f_2$	nc	7.350	4.534	2.860	8.66	nc	120
$4f_1$	$12k$	4.671	2.951	1.926	1.265	⋯	−33.57	−40
$4f_2$	$12k$	4.480	3.072	2.017	1.317	3.15	−39.90	−40

tron correlation. As far as magnetism is concerned, the alkali metal ions play a passive role, the corresponding states being far from the Fermi level; the fact that Sr hexaferrite was considered in Ref. 3 is likely to be insignificant, more important may be the difference of the crystal parameters. Taking all these differences into account, the LSW method seems to work surprisingly well. Despite the poor description of the strong electron correlation by LSDA the gap $\approx$0.63 eV was obtained. The energy differences between the excited and ground state spin configurations come out similar to our results for the smallest U value, in particular their sequence is, with one exception, the same (Table IV).

TABLE V. The intrasublattice exchange interactions. Energy differences $\Delta(U)$ in eV are between excited spin arrangement (inverted spins of iron sublattices s_1, s_2) and the ground state.

s_1	s_2	$\Delta(3.47)$	$\Delta(6.94)$	$\Delta(10.41)$
$2f_1'$	⋯	1.768	1.112	0.746
$2f_1''$	⋯	1.768	1.112	0.746
$2f_1'$	$2f_1''$	3.648	2.251	1.512
$2f_2'$	⋯	1.740	1.080	0.695
$2f_2''$	⋯	1.740	1.080	0.695
$2f_2'$	$2f_2''$	3.544	2.190	1.392
$8k'$	⋯	2.269	1.567	1.063
$4k''$	⋯	0.798	0.636	0.464
$8k'$	$4k''$	4.319	2.765	1.798

An important conclusion follows from Table II and Fig. 2—once the distance between the Fe ions is large [$r_{ij}>0.5$ nm, $(i,j)\equiv(a,b),(a,f_2),(b,f_1)$] the exchange integrals are small. This justifies the limitation of the present analysis, in which the interactions between the nearest neighbors were taken into account and the next-nearest neighbors were considered only if the Fe—Fe distance was smaller than 0.4 nm.

Virtually all exchange integrals are positive, i.e., the exchange is in our convention antiferromagnetic. As seen from Figs. 2 and 3 in all cases J_{ij} decrease as the onsite Coulomb repulsion parameter U increases. This can be expected: the leading interaction in ferrites is believed to be the superexchange and in the simple Anderson picture corresponding exchange integrals are proportional to b^2/U, where b is the transfer integral.[15] On the other hand, the $J_{ij}(U)$ decrease is slower than the Anderson theory predicts, pointing to the fact that the oxygen states play an active role and that other exchange mechanisms cannot be neglected. Of interest is the $4f_1$-$4f_2$ interaction—in this case the exchange path is complicated, as the iron ions in question do not share a common oxygen neighbor. Despite this fact, the exchange integral comes out as medium large.

We used the complete set of the 13 calculated J_{ij} to determine the Curie temperature. In the molecular field approximation[2] the Curie temperature corresponds to the largest eigenvalue of the complete 24×24 matrix of exchange interactions (The Bravais unit cell contains 24 sites of iron atoms) multiplied by the number of equivalent neighbors. In the molecular field approximation the fluctuation of spins is neglected, the system is artificially made more stable, and, as a consequence, the transition temperature is overestimated. The fluctuation of spins is taken into account in RPA, but until now this method was applied to simple magnetic systems only. We did extend the RPA to structurally complex materials (the details will be presented elsewhere,[16] but a brief summary of the approach is given in the Appendix). In Fig. 4 we show critical temperatures calculated within both MFA and RPA. Experimental value is drawn as a horizontal bar (its height corresponds to the span of experimental data). The reduction obtained by RPA for a

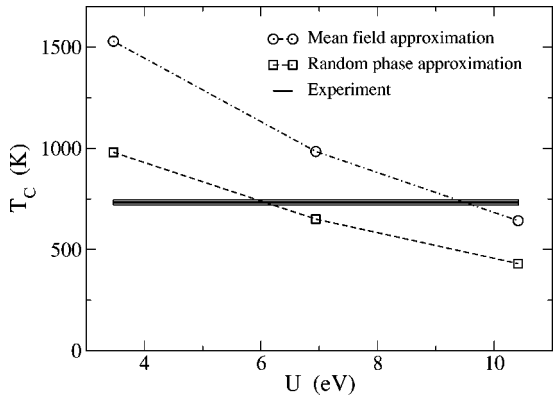

FIG. 4. The Curie temperature calculated from inter- and intrasublattice J_{ij} using the molecular field approximation and random phase approximation. The horizontal bar corresponds to the range of experimental values (Ref. 1).

single sublattice ferromagnet with spin 5/2 and $z=6$ interacting neighbors is substantial $T_C^{RPA}/T_C^{MFA}=2/3$.[2] This approximately holds also for our much more complicated structure. Taking MFA as an upper bound and RPA as a lower bound, we can conclude that the experimental critical temperature is reproduced by calculations for U in the range from 6 to 7 eV. This result is in agreement with the general experience concerning the strength of the intraatomic Coulomb correlations in iron compounds.

VI. CONCLUSIONS

Our results show that the calculations based on DFT are capable to describe the exchange interaction in the complex iron oxides. The method we used employs differences of the total energy of different collinear spin configurations. Its success depends crucially on the fact that the electronic structure of all configurations corresponds to an insulator—the reversal of the spin then leads to a small change of the electronic states only. In order to obtain the insulating state, the GGA +U method had to be used. The calculations do not allow us to identify contributions of different mechanisms to the exchange integrals, but from the $J_{ij}(U)$ dependence we can conclude that the leading mechanism is the antiferromagnetic superexchange.

ACKNOWLEDGMENTS

This work was supported by the project A1010214 of the Grant Agency of the AS CR, by the research program MSM0021620834.

APPENDIX: CALCULATION OF THE CRITICAL TEMPERATURE—RANDOM PHASE APPROXIMATION

The RPA formalism is based on Green's function technique. We define the (retarded) Green's function (analogically to Callen[17])

$$G_{ij}^{AB}(a;\tau) = -\frac{i}{\hbar}\Theta(\tau)\langle[\hat{s}_{i,A}^{+}(\tau), \exp(a\hat{s}_{j,B}^{z})\hat{s}_{j,B}^{-}]\rangle, \qquad \text{(A1)}$$

where a is an auxiliary parameter and $[\hat{X},\hat{Y}]=\hat{X}\hat{Y}-\hat{Y}\hat{X}$ is a commutator. Here $\hat{s}_{i,A}^{\pm}=\hat{s}_{i,A}^{x}\pm i\hat{s}_{i,A}^{y}$ and $\hat{s}_{i,A}^{z}$ are spin operators operating in the unit cell i at basis site A; their time dependence is understood within the Heisenberg picture. $\Theta(\tau)$ is a step function, i.e., $\Theta(\tau)=1$ for $\tau\geqslant 0$, zero otherwise. Mean value in the equation (A1) means $\langle\hat{A}\rangle=\mathrm{Tr}[\rho\hat{A}]=\mathrm{Tr}[\exp(-\beta\hat{H})\hat{A}]/\mathrm{Tr}[\exp(-\beta\hat{H})]$ with $\hat{H}$ being the Heisenberg Hamiltonian and $\beta=1/k_BT$ with k_B being the Boltzmann constant and T a temperature.

The equation of motion for the Green's function (A1) can be simplified by applying the RPA decoupling according to Tyablikov.[18] Time and lattice Fourier transformations allow then to express the Green's function explicitly in the following form,

$$G_{AB}(\omega,\mathbf{q}) = \frac{1}{2\pi}\langle[\hat{s}_{i,A}^{+}, \exp(a\hat{s}_{j,A}^{z})\hat{s}_{j,A}^{-}]\rangle\{[\hbar\omega\mathbb{1} - \mathbf{N}(\mathbf{q})]^{-1}\}_{AB}, \qquad \text{(A2)}$$

where $\mathbb{1}$ is unity matrix and

$$N_{AB}(\mathbf{q}) = \delta_{AB}\sum_{C} J_{AC}(\mathbf{0})\langle\hat{s}_C^z\rangle - \langle\hat{s}_A^z\rangle J_{AB}(\mathbf{q}). \qquad \text{(A3)}$$

Application of the fluctuation-dissipative theorem leads to a set of decoupled differential equations in variable a of the type solved by Callen [see Eq. (44) in Ref. 8]. From their solution in the limit $T\to T_C$ we obtain a set of self-consistent equations for mean values of moments

$$\langle\hat{s}_A^z\rangle = \frac{2S_A(S_A+1)}{3k_BT_C}\left(\frac{1}{\Omega}\int d\mathbf{q}[\mathbf{N}^{-1}(\mathbf{q})]_{AA}\right)^{-1}, \qquad \text{(A4)}$$

which can be solved by iterative methods. Together with the self-consistent set of $\langle\hat{s}_A^z\rangle$ we obtain critical temperature T_C, Eq. (A4).

*Electronic address: novakp@fzu.cz

[1] H. Kojima in *Ferromagnetic Materials*, edited by E. P. Wohlfarth, (Nort-Holland, Amsterdam, 1982), Vol. 3.
[2] J. S. Smart, *Effective Field Theories of Magnetism* (W.B. Saunders Company, San Francisco, 1966).
[3] C. M. Fang, F. Kools, R. Metselaar, G. de With, and R. A. de Groot, J. Phys.: Condens. Matter **15**, 6229 (2003).
[4] P. W. Anderson, in *Magnetism*, edited by G. T. Rado and H. Suhl (Academic Press, New York, 1963), Vol. 1, p. 25.
[5] X. Obradors, A. Collomb, M. Pernet, D. Samaras, and J. C. Joubert, J. Solid State Chem. **56**, 171 (1985).
[6] P. Blaha, K. Schwarz, G. K. H. Madsen, D. Kvasnicka, and J. Luitz, *WIEN2k, An Augmented Plane Wave + Local Orbitals Program for Calculating Crystal Properties*, Karlheinz Schwarz, Techn. Universtät Wien Austria, 2001. ISBN 3-9501031-1-2.
[7] D. Singh, *Plane Waves, Pseudopotentials and the LAPW Method* (Kluwer Academic, Dordrecht, 1994).
[8] J. P. Perdew, K. Burke, and M. Ernzerhof, Phys. Rev. Lett. **77**, 3865 (1996).
[9] J. P. Perdew and Y. Wang, Phys. Rev. B **45**, 13 244 (1992).
[10] Z. Yang, Z. Huang, L. Ye, and X. Xie, Phys. Rev. B **60**, 15674 (1999).
[11] I. Solovyev, N. Hamada, and K. Terakura, Phys. Rev. B **53**, 7158 (1996).
[12] R. Zimmerman, P. Steiner, R. Claessen, F. Reinert, S. Hüfner, P. Blaha, and P. Dufek, J. Phys.: Condens. Matter **11**, 1657 (1999).
[13] A. I. Liechtenstein, V. I. Anisimov, and J. Zaanen, Phys. Rev. B **52**, R5467 (1995).
[14] G. K. H. Madsen and P. Novák, Europhys. Lett. **69**, 777 (2005).
[15] P. W. Anderson, Phys. Rev. **115**, 2 (1959).
[16] J. Rusz, I. Turek, and M. Diviš, Phys. Rev. B **71**, 174408 (2005).
[17] H. Callen, Phys. Rev. **130**, 890–898 (1963).
[18] S. V. Tyablikov, Ukr. Mat. Zh. **11**, 287 (1959); *Methods of Quantum Theory of Magnetism* (Plenum Press, New York, 1967).